NASA TECHNICAL NOTE

NASA TN D-4925

NASA TN D-4925

A RADIOMETER FOR USE IN THERMAL STUDIES OF SPACECRAFT

by George E. Sweet and Howard B. Miller

Langley Research Center
Langley Station, Hampton, Va.

NATIONAL AERONAUTICS AND SPACE ADMINISTRATION • WASHINGTON, D. C. • DECEMBER 1968

NASA TN D-4925

A RADIOMETER FOR USE IN THERMAL STUDIES OF SPACECRAFT

By George E. Sweet and Howard B. Miller

Langley Research Center
Langley Station, Hampton, Va.

NATIONAL AERONAUTICS AND SPACE ADMINISTRATION

For sale by the Clearinghouse for Federal Scientific and Technical Information
Springfield, Virginia 22151 – CFSTI price $3.00

A RADIOMETER FOR USE IN THERMAL STUDIES OF SPACECRAFT

By George E. Sweet and Howard B. Miller
Langley Research Center

SUMMARY

A new disk radiometer that is essentially a modification of a loss-measuring slug transducer has been designed for space vacuum-thermal environmental studies. The device is operable in vacuums less than 1.3×10^{-3} N/m^2 at ambient temperature levels from 80° K to 450° K. Both steady-state and time-varying total irradiances with magnitudes between 200 and 1500 W/m^2 can be measured with an error of about 10 percent. Once the radiometer is calibrated by using an extended black-body reference source, it can be used in a variety of thermal study situations without recalibration. Because it is small in size (2.3-cm diameter by 0.5-cm height) and external-cooling or constant-temperature references are not required, it effects a minimal thermal disturbance to the test surface. The major feature of this radiometer is a shield which is located between the sensor and mounting surface. This shield is instrumented so that an empirical correction can be applied to the radiometer measurements to compensate for unwanted heat transfer between the sensor and mounting surface. Criteria are presented for designing the sensor so that it will remain in temperature equilibrium with relevant heat sources and thus simplify data reduction. Example applications of the radiometer to a thermal-control balloon model are also presented.

INTRODUCTION

A radiometer was required to measure steady-state and time-varying total irradiances in the range of 200 to 1500 W/m^2 at the surfaces of spacecraft and models of spacecraft under vacuum conditions (pressures less than 1.3×10^{-3} N/m^2). When the radiative and conductive components of heating can be separated at the test surfaces, the results of thermal tests can be more rapidly evaluated. This separation is particularly beneficial for complex configurations where multiple reflections and emissions occur. For such applications a radiometer with the following characteristics is desirable:

(1) Small physical dimensions to minimize shadowing effects

(2) Low thermal mass to minimize thermal disturbances to the test surfaces

(3) Capability of indicating irradiances when the mounting-surface temperature is appreciably different from that of the radiometer

(4) Capability of maintaining a constant calibration irrespective of the mounting method

(5) Good constancy of calibration between radiometers

A radiometer meeting all these requirements could not be found. Some slug radiometers are described in references 1 and 2. Radiometers of this type generally have large thermal masses and are subject to error for measurements of steady-state irradiances. Gradient radiometers, although capable of measuring time-varying irradiances, require massive heat sinks (ref. 1). The radiometer described in reference 3 overcomes many of the disadvantages of other designs but is impractical for use in irradiance mapping because of its thermal mass and sophisticated electronics.

The present paper presents design parameters for constructing what is essentially a total loss-measuring slug transducer. The loss-measuring principle is based upon the fact that signal errors are proportional to temperature differences between the sensing element and radiometer case. In the present radiometer an instrumented shield located between the sensor and the mounting surface is analogous to the case of a conventional loss-measuring device. This radiometer is different from most slug transducers in that it is small (2.3-cm diameter by 0.5-cm height) and its components have a low thermal mass. As a result, for many applications the sensor remains in thermal equilibrium with the relevant heat sources, and data reduction is simplified.

Calibration data are included herein for several prototype radiometers for two simulated mounting conditions. Tests for response to time-varying irradiance, angular sensitivity, and the application of this radiometer to a passive thermal-control balloon model are also presented.

SYMBOLS

C	radiometer correction, $k\left(T_d - T_b\right) + C'$
C'	displacement of correction curve from coordinate axis
c	specific heat
E	energy
$F_{a,d}$	source-sensor view factor

$F_{b,d}$	shield-sensor view factor
H	irradiance
H_e	equivalent black-body irradiance of heat sources
k	slope of the radiometer correction curve C, $\frac{T_e - T_d}{T_d - T_b}$
M	constant, $\frac{c\gamma\tau}{\epsilon}$
S	surface area
T	temperature
T_e	equivalent black-body temperature of heat sources, $\left(\frac{H_a}{\sigma}\right)^{1/4}$
t	time
$\frac{dT}{dt}$	slope of time-temperature curve
α	absorptance
γ	density
ϵ	emittance
θ	angle between radiation source and normal to radiometer
σ	Stefan-Boltzmann constant
τ	thickness

Subscripts:

a	heat source
B	bottom
b	radiometer shield

d	radiometer sensor
m	mounting surface
T	top
w	wall

RADIOMETER DESCRIPTION

The signal output of a loss-measuring radiometer is dependent on the case temperature, that is, the signal is affected by heat transfer between the case and the sensing element. The case of the loss-measuring slug transducer is instrumented to measure temperature differences between the case and the sensor. These temperature differences are proportional to the signal error induced by the unwanted heat transfer between these elements. In the present device an instrumented shield, analogous to a radiometer case, is used to provide this information. In the following sections an empirical correction for radiometer errors is introduced, an error analysis is presented, and the sensor temperature response described.

Principle of Operation

The principle of operation of the present radiometer is similar to that of a slug radiometer (ref. 1). The following sketch shows a representative radiometer installation with temperature notation as indicated.

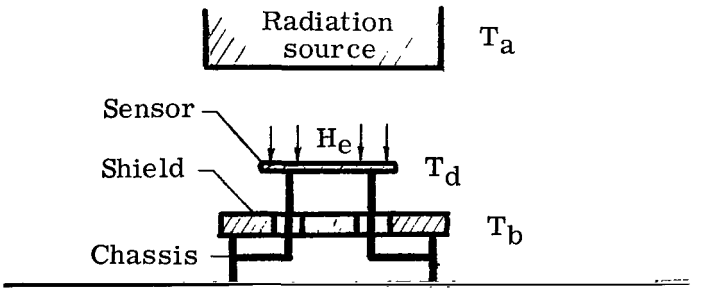

The irradiance at the sensor H_e is $S_a\epsilon_a F_{a,d}\sigma T_a^4$. In many instances the analysis of test data is simplified by considering the source radiation to be originating from an infinite black body. The equivalent irradiance at the sensor is then σT_e^4 where T_e is the temperature of this black body. The general equation for the irradiance at sensor is obtained from the following energy balance:

$$\sum E = 0 = \alpha_d S_d H_e - \epsilon_d S_d \sigma T_d^4 - (c\gamma\tau S)_d \left(\frac{dT}{dt}\right)_d + \text{Net radiative and conductive heat transfer between sensor and shield} \quad (1)$$

The principal feature of the present radiometer is the shield which is interspaced between the sensor and the mounting surface. This shield intercepts most of the radiant and conductive heat transfer between the sensor and the mounting surface. The magnitude of this unwanted heat transfer is then proportional to $T_d - T_b$, the temperature difference between the sensor and the shield. For convenience the last term in equation (1) is introduced as an empirical temperature correction C which is added to the sensor temperature T_d. Hence,

$$H_e = \left(\frac{\epsilon}{\alpha}\right)_d \sigma\left(T_d + C\right)^4 + \left(\frac{c\gamma\tau}{\alpha}\right)_d \left(\frac{dT}{dt}\right)_d$$

If the sensor is assumed to be gray (absorptance α_d is equal to emittance ϵ_d), the equivalent black-body irradiance at the sensor is

$$H_e = \sigma\left(T_d + C\right)^4 + M_d \left(\frac{dT}{dt}\right)_d \quad (2)$$

where M_d is a constant for the radiometer sensor. At solar wavelengths the assumption of a gray sensor will introduce small errors of about 2 percent. Separate calibrations should be carried out at these wavelengths and optical-property measurements should not be depended on. Equation (2) is similar to that of the slug-radiometer equation given in reference 1. The present radiometer is different in that the sensor constant M_d is much smaller than that of some slug designs (ref. 2). This difference causes the present device to attain thermal equilibrium with radiant sources more quickly than other slug designs. As a result, the sensor will remain essentially in equilibrium with the slowly changing radiance of spacecraft surfaces. Equation (2) then simplifies to

$$H_e = \sigma\left(T_d + C\right)^4 \quad (3)$$

The black-body temperature of the source is

$$T_e = \left(\frac{H_e}{\sigma}\right)^{1/4} = T_d + C \quad (4)$$

The empirical correction C is obtained by correlating calibration data with sensor-shield temperature differences.

Error Analysis

Expressions for determining the radiometer error as a function of thermocouple measuring accuracy and of k the slope of the correction curve are presented. The error in measuring an irradiance H_e is

$$\text{Percent error } H_e = \frac{\Delta H_e}{H_e} \times 100 \tag{5}$$

The approximate error ΔH_e for transient irradiances may be obtained from equation (2) by substituting $k(T_d - T_b) + C'$ for C and taking increments. By substituting this result into equation (5), the error is obtained as

$$\text{Percent error } H_e = \frac{4\sigma(T_d + C)^3\left[\Delta T_d + k(\Delta T_d + \Delta T_b) + \Delta C + \Delta C'\right] + M\Delta\left(\frac{dT}{dt}\right)_d}{H_e} \times 100 \tag{6}$$

where ΔC and $\Delta C'$ are the errors in C attributable to calibrations and ΔT is the practical uncertainty of the radiometer temperature detectors. Noting that $H_e = \sigma T_e^4$ and substituting this equality into equation (6) yields

$$\text{Percent error } H_e = \frac{4(T_d + C)^3\left[\Delta T_d + k(\Delta T_d + \Delta T_b) + \Delta C + \Delta C'\right] + \frac{M}{\sigma}\Delta\left(\frac{dT}{dt}\right)_d}{T_e^4} \times 100 \tag{7}$$

For steady-state irradiances the thermal-mass term is dropped and $T_d + C$ becomes equal to T_e (eq. (4)). The error is

$$\text{Percent error } H_e = \frac{4\left[\Delta T_d + k(\Delta T_d + \Delta T_b) + \Delta C + \Delta C'\right]}{T_e} \times 100 \tag{8}$$

The percent error, expressed in equivalent black-body temperature, may be found by noting that the numerator in equation (8) is $4\Delta T_e$. Then

$$\text{Percent error } T_e = \frac{\text{Percent error } H_e}{4} \tag{9}$$

Sensor Temperature Response

For an isolated sensor that exceeds the source temperature by a small amount $T_d - T_e$, the time required to cool from $T_{d,1}$ to $T_{d,2}$ can be determined by

linearizing equation (2). By substituting σT_e^4 for H_e and considering the correction C small, equation (2) may be written as

$$0 = -\sigma\left(T_e^4 - T_d^4\right) + M_d\left(\frac{dT}{dt}\right)_d \tag{10}$$

For small temperature differences, $T_e^4 - T_d^4$ is approximately equal to $4T_e^3\left(T_e - T_d\right)$. Substituting this relation into equation (10) and solving for dt_d yields

$$dt_d = -\frac{M_d}{4\sigma}\frac{dT_d}{T_e^3\left(T_d - T_e\right)} \tag{11}$$

By integrating equation (11) the time required for the sensor to cool from $T_{d,1}$ to $T_{d,2}$ is obtained.

$$t = \frac{M_d}{4\sigma T_e^3}\log_e\frac{T_{d,1} - T_e}{T_{d,2} - T_e} \tag{12}$$

For an equivalent black-body temperature of 400° K, a radiometer sensor representative of the present design $\left(M_d = 350\ J/m^2\text{-}K^\circ\right)$ would require about 55 seconds to cool from 410° K to 401° K. For $T_e = 300^\circ$ K, the time to cool the same amount would be $\left(\frac{400}{300}\right)^3 \times 55$ or 130 seconds. The time required for the temperature to decay $1/e$ of a small increment $T_d - T_e$ is $\frac{M_d}{4\sigma T_e^3}$. For $T_e = 400^\circ$ K, this decay would take about 24 seconds and for $T_e = 300^\circ$ K, about 57 seconds. Although these response rates are slow, many radiation sources encountered in spacecraft testing also change temperature slowly. Criteria for determining whether the sensor response rate is sufficiently rapid to ignore the thermal-mass term in equation (2) are presented in the appendix. In order that the correction C not be influenced by mass effects, the temperature response for the sensor and shield should be made equal.

DESIGN AND CONSTRUCTION

In this section the method used to construct the prototype radiometers for operation in an environment ranging from 80° K to 450° K is described. Figure 1 shows the radiometer components which include a plastic chassis and thermocouple-instrumented sensor and shield. The assembled radiometers were 0.5 cm in height and 2.3 cm in diameter with mounting lugs included. The results of tests and calibrations indicated several construction refinements that could be incorporated in future models. These refinements are discussed in a later section.

Sensor

The sensor was made from a 0.0076-cm-thick (3-mil) silver disk which was 1.27 cm in diameter. The side of the sensor facing the shield was gold-plated to minimize radiant heat transfer between these two components. The disk was embossed to increase its rigidity. A thermocouple fabricated from No. 40 chromel-alumel wire was welded to an indentation in the center of the disk. Electron-beam welding was chosen to insure a good electrical connection at the thermocouple junction and good thermal contact. To increase response with respect to the relevant heat sources, the top surface of the sensor was painted with 3M 401-C 10 flat black epoxy paint. Reflectance measurements indicate that in the spectral region between 1 and 25 μm, this coating had an emittance of 0.95. The solar absorptance-emittance ratio was about 1.02. To minimize error by conduction loss, the thermocouple leads were routed across and close to the top surface where they would be warmed by the source radiation and would be essentially the same temperature as the sensor.

Shield

The shield was made from a 0.0051-cm-thick (2-mil) stainless-steel disk which was 1.9 cm in diameter. The optical coatings and method of thermocouple attachment were the same as those for the sensor. This disk was mounted on the chassis 0.24 cm beneath the sensor.

The shield, which is larger than the sensor, serves several important functions. Primarily, it blocks most of the radiant heat transfer between the sensor and the mounting surface. It also receives part of the irradiance to be measured and seeks to attain temperature equilibrium with the source. As a result, error-producing thermal gradients between the sensor and shield are small. Perhaps the most important function of the shield is to provide temperature information indicative of the magnitude of unwanted heat transfer between the sensor and mounting surface. An empirical correction C (eq. (3)) is determined by correlating radiometer calibration data with the temperature differences between the sensor and shield.

For the measurement of time-varying irradiance, both the sensor and the shield should be designed to cool or heat at the same rate. Because the sensor shadows part of the shield from the source radiation, the shield constant M_b must be less than M_d for the sensor. Thus, for equal cooling rates

$$M_b = M_d\left(1 - F_{b,d}\right)$$

The prototype radiometers were not intended to measure rapid transient irradiances, and M_b was about twice $M_d\left(1 - F_{b,d}\right)$.

Chassis

The chassis (see fig. 1) was injection molded from a polytetrafluorethylene plastic. This material was chosen because of its low thermal conductivity, good dimensional stability, and low outgassing between 100° K and 500° K. The chassis was designed to provide a long thermal path between the sensor attachment point and the mounting feet. The parts of the chassis facing the mounting surface were vapor deposited with gold to minimize radiant heat transfer between the chassis and the mounting surface. The remaining parts were left uncoated to promote rapid cooling or heating. The low-temperature emittance of the uncoated parts was about 0.8.

The sensor and shield were attached to the chassis by mushrooming the ends of the locating pins with a warm soldering iron. The No. 40 chromel-alumel thermocouple wires leading from the sensor and shield were attached to No. 36 chromel-alumel extension wires. These, in turn, were secured to the radiometer by lead-wire supports molded onto the chassis.

APPARATUS AND PROCEDURES

The radiometers were calibrated to determine the radiometer correction C. They were also tested to determine their accuracy in measuring time-varying irradiances and angular sensitivity with respect to a collimated heat source. These calibrations and tests were conducted at a pressure less than 1.3×10^{-3} N/m^2 in the 5-foot-diameter, 5-foot-long vacuum system at the Langley Research Center. Strip-chart recorders were used for all temperature measurements.

Calibration Apparatus

The calibration apparatus as installed in the vacuum chamber is shown in figure 2. A heated plate of known radiant power was used as the calibration source. A temperature-controlled mounting surface was used as a second heat source to simulate unwanted heat transfer between the radiometer and its supporting surface. This second heat source was used in a different way for each of the two sets of calibrations. First, the radiometer was mounted directly on the heat source to simulate conductive heat transfer between the radiometer and a mounting surface. Second, the radiometer was suspended slightly above this heat source to simulate radiant heat transfer. In order to minimize the effect of heat-source radiation reflected from the chamber walls to the radiometer, the entire wall area surrounding the test apparatus was cooled with liquid nitrogen.

The calibration source was made from a 0.63-cm-thick copper disk, 25.4 cm in diameter. Its temperature was controlled by passing heated or cooled nitrogen vapors through a copper coil attached to the rear surface of the disk. In an attempt to increase

the effective emittance, the side of the source facing the radiometer was machined to produce a surface covered with miniature pyramids. To determine the uniformity of temperature distribution, the peak of one pyramid and the base of each of five pyramids located in a radial pattern were instrumented with thermocouples made of No. 40 chromel-alumel wire. This surface was then coated with 3M 401-C 10 flat black epoxy paint.

The reflectance of the calibration surface was measured by using two samples, which were prepared at the same time. The results of these measurements indicated an emittance of 0.96 for one sample whereas an emittance of 0.935 was indicated for the other sample. An examination of the samples indicated that these differences were probably due to a nonuniform application of the paint. Flat samples, also coated with the 3M paint, indicated an emittance of 0.95. For the present tests, the average emittance of the calibration source was assumed to be 0.95.

The temperature-controlled mounting surface was built to simulate conditions which might be experienced by a radiometer mounted on a variable-temperature surface. This surface consisted of a 2.54-cm-diameter copper disk attached to a soldering iron. Energy transfer to the radiometer was controlled by operating the mounting surface at various temperature levels. The two mounting positions of the radiometer with respect to the mounting surface are shown in figure 3. For the suspended-mounting tests, the mounting surface was painted black to make the background heat transfer radiative. For the surface-mounting tests, the paint was removed and the exposed copper substrate caused the heat transfer to be predominantly conductive. In both cases a clearance of 1 cm was maintained between the sensor and calibration source.

Method of Calibration

A series of calibration-source and radiometer-shield temperatures were recorded with the sensor temperature T_d held constant at 250° K, 300° K, 350° K, and 400° K. These constant temperatures were maintained by manipulating the heat controls for the calibration source and mounting surface to elevate successively the background radiation while lowering the calibration-source temperature. The temperature difference between T_e and T_d is equal to the correction C in equation (2) and $T_e = T_a\left(\epsilon_a \times F_{a,d}\right)^{1/4}$. The view factor for these calibrations was 0.998 ± 0.001. This correction C was plotted against the temperature difference between the sensor and shield to form curves of constant sensor temperature. (See fig. 4.) For a given sensor temperature and known temperature difference between the sensor and shield, the correction C is obtained as indicated by the dashed lines. When this correction is added to the sensor temperature, the equivalent black-body temperature T_e of the irradiance at the radiometer sensor, as indicated by equation (3), is obtained. Although these data were recorded while the

calibration source was cooling by radiation to the liquid-nitrogen-cooled walls, the radiometer constant M_d was much less than $(c\gamma\tau)_a$ of the calibration source; therefore, the thermal-mass term in equation (2) is negligible, and the cooling effect can be neglected. (See appendix.) The accuracy of the corrections ΔC is $\Delta\left[\left(\epsilon_a F_{a,d}\right)^{1/4} T_a\right] + \Delta T_d$. For the present calibrations ΔC was primarily dependent on temperature-measurement accuracy which was about $\pm 2^\circ$ K. The error in ΔC was therefore about $\pm 4^\circ$ K.

Time-Varying-Irradiance Test

The object of the time-varying-irradiance test was to compare and evaluate the two methods of data reduction (eqs. (2) and (3)). The apparatus and method of supporting the radiometer are shown in figure 2. The radiometer and calibration source were first cooled to about 190° K. Then heated nitrogen gas was used to raise the temperature of the calibration source rapidly to about 400° K. Heat was not applied to the mounting surface for these tests.

Angular-Sensitivity Test

A radiometer, mounted on the center of a 30-cm-square plate, was placed inside a vacuum chamber with an effective black-body wall temperature of 180° K. Simulated solar energy produced by a carbon arc was allowed to pass through a chamber window and strike the radiometer as it was progressively rotated from 0° to 90°. For comparative purposes, two mounting surfaces with different optical properties were used. All measurements were recorded as a function of angular displacement from the simulator axis. For these tests a second radiometer, similar to the one being tested, was mounted normal to the radiation source and used to monitor the constancy of the solar-simulator radiation.

DISCUSSION OF RESULTS

Calibrations

Figure 5 shows calibration results for both suspended- and surface-mounted radiometers for a constant sensor temperature of 300° K. Within the accuracy of the present calibrations, these results indicate that some basic design objectives were met; that is, a good constancy of calibration existed between individual radiometers, and the mounting method produced a negligible effect on the calibrations. For these tests the mounting-surface temperatures ranged from 260° K to 640° K. Figure 6 shows that the radiometer response is relatively insensitive to simulated mounting-surface temperatures over a wide temperature range. For example, for a mounting-surface temperature 160° K greater than that of the sensor, the correction was only -4° K.

At a sensor temperature of 300° K, the average calibration curve passed about 1.5° K above the intersection of the coordinate axes. (See fig. 5.) This trend was more predominant at the higher sensor temperatures (2° K at 350° K, and 2.5° K at 400° K). Ideally, when the sensor and shield temperatures are equal, no correction should be needed because there would be no net heat transfer between the elements. In actuality, the sensor-shield view factor was less than one, about 0.9, and some heat transfer did occur between the sensor bottom and the liquid-nitrogen-cooled walls. Also, the calculated T_e may have been too large because the exact emittance of the calibration source was unknown.

Because these conditions did not fully account for the measured displacements, several of the test radiometers were dismantled. A microscopic examination of the gold-plated surfaces revealed that in numerous places the embossing dies had exposed the silver substrate, and it was now tarnished. Reflectance measurements indicated emittances between 0.2 and 0.3, an order of magnitude greater than expected. Thus, radiant heat transfer from the underside of the sensor to the nitrogen-cooled walls $\left(0.1\epsilon_{dB}\sigma T_d^4\right)$ was about ten times greater than anticipated.

Calibration curves calculated from the measured emittance and with only radiant heat transfer considered are compared with the measured curve for a sensor temperature of 300° K in figure 7. The calculated curves indicate that a vertical displacement would increase as the emittance of the underside of the sensor increased. To minimize this displacement, one of the test radiometers was modified by bonding a 0.0076-cm-thick (0.3-mil) gold disk to the underside of the sensor $\left(\epsilon_{dB} \approx 0.03\right)$. In figure 8 the calculated and measured calibration curves are compared for this modified radiometer for a constant sensor temperature of 300° K. This figure indicates that both the displacement and the magnitude of the correction C were reduced.

Differences between the measured and calculated curves are indicative of the part of the correction that is due to conduction and approximations in analysis. Calibration curves for this radiometer at other temperatures are compared in figure 9. The upward displacement of these curves from the intersection of the coordinate axes is still present at the higher temperatures. These displacement errors, although small, can be reduced by increasing the sensor-shield view factor.

By using the slopes of the calibration curves presented in figure 9 and an assumed thermocouple uncertainty of ±2° K, the expected radiometer error was calculated from equations (8) and (9). The results are summarized in the table at the top of page 13. Calibration uncertainties contributed to more than half of the errors listed in this table. These errors could be significantly reduced by employing precision potentiometers during calibrations.

Incident irradiance, H_e, W/m^2	Equivalent black-body temperature, T_e, ^oK	Percent error in –	
		H_e	T_e
220	250	10.7	2.7
460	300	9.7	2.4
850	350	8.3	2.1
1450	400	7.0	1.7

Time-Varying Irradiance

The object of the time-varying-irradiance test was to show the applicability of equation (3). Figure 10 presents a comparison of the temperature response of the radiometer sensor and shield to a rapid rise in the equivalent black-body temperature of the calibration source. The maximum rate of source temperature change was 34^o K per minute and occurred at 3 minutes after the start of the test. This rate diminished to about 3^o K per minute after 14 minutes. Although these rates of change are arbitrary, they are believed to encompass most of the irradiances and rates of change of irradiances that would be encountered in spacecraft testing. One exception was that the radiometer would not respond rapidly enough to measure the transient radiance from a solar simulator that was suddenly turned on.

The sensor and shield constants M_d and M_b were not equal for the radiometer tested. The sensor constant M_d was calculated to be 350 J/m^2-^{o}K, and the shield constant M_b was 630 J/m^2-^{o}K. After 5 minutes, however, the rates of heating for these elements became essentially equal and the differences between the constants probably did not significantly affect the reduced data. Compare the slopes of the sensor and shield curves in figure 10.

Figure 11 shows the differences between equivalent calibration-source temperatures T_e and corrected radiometer readings. The radiometer readings were corrected in two ways: first, by merely adding the correction C to T_d (eq. (3)); and second, by adding C to T_d and including the thermal-mass term (eq. (2)). The fact that the corrected radiometer data do not eventually equal the equivalent black-body temperature of the source T_e (14 minutes and beyond) is attributed to experimental error and is within the accuracy of the device. Of greater importance is a comparison between the two methods of data reduction. At 11 minutes the error resulting from the use of equation (3) rather than the use of equation (2) is only about 1^o K (about 1.5-percent difference in energy). Here the rate of change of the equivalent temperature of the calibration source was about 4^o K per minute. When the source rate of change of temperature is greater than 4^o K per minute, the thermal-mass term should be included.

Angular Sensitivity

Figure 12 presents differences between corrected radiometer readings and the effective black-body temperature of the incident irradiance T_e for several angular positions with respect to a solar simulator. For these tests a second radiometer, similar to the one being tested, was mounted normal to the radiation source and used to monitor the constancy of the solar-simulator radiation. The effective black-body temperature of the source is expressed as

$$T_{e,source} = \left\{\left[(T_d + C)_{monitor}^4 - T_{e,w}^4\right]\cos\theta + T_{e,w}^4\right\}^{1/4}$$

where $T_{e,w}$ was the effective black-body temperature of the vacuum-chamber walls.

These tests were made with the test radiometer mounted on both black and aluminum surfaces. Neither the temperatures of nor the reflections coming from the mounting surfaces had an appreciable effect on these results. (See fig. 12.) At angles approaching 90^o, the radiometer indicated appreciably greater irradiance than the source. This difference was believed to be due to heating of the sensor support posts by the simulator. A small cylindrical guard ring was then placed around the radiometer to prevent direct simulator radiation from striking these posts. The outside of the ring was painted black. To minimize the radiant heat transfer from the guard ring to the sensor, the inside of the ring was made shiny ($\epsilon = 0.03$). Unfortunately, the guard ring was taller than necessary and the sensor was partially shielded from the simulator radiation. This shielding caused the radiometer to indicate a lower than actual irradiance, particularly between 50^o and 80^o. (See fig. 12.) Despite this occurrence, the guard ring improved the radiometer performance, particularly near 90^o.

Improved Radiometer Design

In considering the design and construction of prototype radiometers, two of the most difficult problems would be to construct a sensor with a rapid response and to minimize the effects of strong side radiation on the sensor support posts without increasing the physical dimensions. Turning up the edges of the shield to prevent side radiation from warming the sensor support posts and to increase the sensor-shield view factor was considered. This alteration, however, would have the effect of decreasing the shield temperature response since the mass would be increased and the effective radiating area decreased. Perhaps a better approach would be to space the sensor-shield elements closer together to minimize side radiation effects and to thus increase the view factor.

In the present radiometer the cooling rates of the sensor and shield were not equal, that is, M_b was about twice M_d. To equalize these rates and retain a desirable temperature response the thermal mass of the shield should be decreased. Because the

minimum practical thickness of the shield is believed to be between 0.0051 and 0.0076 cm (2 and 3 mils), the only recourse would be to decrease the thermal mass of the optical coatings on the shield. The black shield coating on the prototype radiometers was about 0.0051 cm thick (2 mils) and accounted for nearly one-half of the shield constant M_b. A newly developed space-stable coating with optical properties comparable to the 3M 401-C 10 flat black epoxy paint is described in reference 4. It is an anodized aluminum blackened by a nickel-sulfide dye which does not significantly increase the thermal mass of the base material. Several sample shields with this coating have been successfully fabricated from 0.0076-cm-thick (3-mil) aluminum. The bottoms of the shields were brush-plated with gold, and the thermocouples were soft-soldered to the gold plating. By using these techniques the sensor and shield could be designed to give equal temperature responses and perhaps improve the radiometer response rate.

RADIOMETER APPLICATIONS TO BALLOON STUDY

The uses and mounting of these radiometers as applied to thermal-vacuum tests of balloon thermal-control enclosures for spacecraft are shown in figure 13. Figure 13(a) shows the opaque balloon model and a radiometer located beside it to monitor the solar-simulator radiance. The purpose of this investigation was to measure the irradiance in areas where a payload would be located within the balloon. A heater was suspended within the balloon to simulate the heat dissipated by the payload. Figure 13(b) shows radiometers mounted along a support bar which was mounted across the balloon diameter. Figure 13(c), an enlargement of part of this bar, shows the radiometers attached to auxiliary mounting annuli which were spot-welded to the bar. Three wire prongs, spot-welded to the annuli, were used to hold the radiometer by its mounting lugs. These auxiliary mounts permit easy radiometer installation on a variety of surfaces. For example, a radiometer for measuring the average balloon α/ϵ ratio was mounted to the inside balloon wall (0.0019 cm (0.75 mil) thick) by this method.

Figure 14 presents representative irradiance measurements along the balloon diameter. Both corrected and uncorrected radiometer data are shown. The high irradiance near the sun-heated side of the balloon is due to the high balloon-wall temperatures in this area. The high irradiance measured at the 70-percent diameter is due to the focusing of heater energy by the balloon walls. The low reading at the 90-percent diameter is due to the opening in the balloon. In most of these data, the radiometer corrections were well within the accuracy of the radiometer, and, therefore, they were not applied.

CONCLUDING REMARKS

Governing parameters for designing a radiometer for use in spacecraft thermal studies are presented. Since this radiometer effects a minimal thermal disturbance on the test surface, a large number may be used to map the irradiance distribution of complex configurations. The feasibility of fabricating these radiometers from materials that are compatible with a space environment has been demonstrated. Representative calibration and performance data show that calibration corrections are relatively insensitive to the method of mounting and to the optical properties and temperature of the mounting surface. In a study of a thermal-control balloon model, application of corrections to the radiometer measurements was found to be unnecessary.

Langley Research Center,
National Aeronautics and Space Administration,
Langley Station, Hampton, Va., July 26, 1968,
124-09-18-06-23.

APPENDIX

RADIOMETER DESIGN CRITERIA FOR SIMPLIFIED DATA REDUCTION

Since radiating surfaces cool or warm cyclically at relatively slow rates in normal spacecraft or model testing, it is possible to design a radiometer that will remain essentially in temperature equilibrium with these surfaces. For such a radiometer, the thermal-mass term $M_d\left(\frac{dT}{dt}\right)_d$ in equation (2) would be negligible, and equation (3) could be used. To determine whether the simplified form is applicable, consideration must be given to the accuracy of the temperature detectors, the anticipated rate of change of the source radiation, and the sensor constant M_d. The following analysis provides a basis for determining when the thermal-mass term of equation (2) can be ignored.

The energy-balance equation for a cooling object is

$$\sum E = 0 = -\epsilon_a \sigma S_a T_a^4 - (c\gamma S\tau)_a \frac{dT_a}{dt}$$

or

$$\frac{dT_a}{dt} = -\left(\frac{\epsilon}{c\gamma\tau}\right)_a \sigma T_a^4 \tag{A1}$$

Similarly, the energy-balance equation for a gray sensor with a view factor of 1 located on a cooling object is

$$\sum E = 0 = \epsilon \sigma S T_e^4 - \epsilon \sigma S T_d^4 - c\gamma S\tau \frac{dT_d}{dt} \tag{A2}$$

The equivalent black-body irradiance from the source and incident to the sensor is σT_e^4; that is, $\sigma T_e^4 = \epsilon_a \sigma T_a^4$.

Multiplying both sides of equation (A2) by dT_a, dividing by ϵ and S, and solving for $\sigma T_d^4\, dT_a$ yields

$$\sigma T_d^4\, dT_a = \sigma T_e^4\, dT_a - \left(\frac{c\gamma\tau}{\epsilon}\right)_d \frac{dT_d\, dT_a}{dt} \tag{A3}$$

By substituting equation (A1) into equation (A3)

$$\sigma T_d^4\, dT_a = \sigma T_e^4\, dT_a + \left(\frac{c\gamma\tau}{\epsilon}\right)_d \left(\frac{\epsilon}{c\gamma\tau}\right)_a \sigma T_a^4\, dT_d$$

is obtained.

Note that the irradiance indicated by the radiometer is $\sigma T_d^4 = H_d$, and that the actual incident irradiance is $\sigma T_e^4 = \epsilon_a \sigma T_a^4 = H_e$. Solving for the indicated irradiance H yields

$$\left.\begin{aligned} H_d\, dT_a &= \left[H_e\, dT_a + H_e\left(\frac{c\gamma\tau}{\epsilon}\right)_d\left(\frac{1}{c\gamma\tau}\right)_a dT_d\right] \\ H_d &= H_e\left[1 + \left(\frac{c\gamma\tau}{\epsilon}\right)_d\left(\frac{1}{c\gamma\tau}\right)_a \frac{dT_d}{dT_a}\right] \\ H_d &= H_e\left[1 + \frac{M_d}{(c\gamma\tau)_a}\frac{dT_d}{dT_a}\right] \end{aligned}\right\} \quad \text{(A4)}$$

When the source is cooling, the rate of sensor cooling will approach that of the source and $\frac{dT_d}{dT_a}$ will approach 1. Thus, for small ratios of $\frac{M_d}{(c\gamma\tau)_a}$, the irradiance as indicated by the radiometer is approximately $H_d \approx H_e$. For many thermal model and spacecraft tests, H_d as indicated by the radiometer will be equal to H_e within the accuracy of the temperature-detecting devices. For accurate measurement by thermocouples, the radiometer constant M_d should be about one twenty-fifth of $(c\gamma\tau)_a$. When rapid transient irradiances, such as the irradiance from a rapid-rise electric heater, must be measured, equation (2) must be used.

REFERENCES

1. Stempel, F. C.; and Rall, D. L.: Direct Heat Transfer Measurements. ISA J., vol. 11, no. 4, Apr. 1964, pp. 68-73.

2. Gilcrest, A. S.; and Mon, G. R.: A Calorimeter for Determining Thermal Radiation Fluxes in Space Simulation Chambers. Annu. Tech. Meeting Proc., Inst. Environ. Sci., 1963, pp. 369-376.

3. Kendall, James M., Sr.; and Plamondon, Joseph A.: An Absolute Cavity Radiometer for the Measurement of Thermal Radiation. AIAA/IES/ASTM Space Simulation Conference, Sept. 1966, pp. 179-184.

4. Wade, William R.; and Progar, Donald J.: (With appendix by Donald H. Humes): Effects of a Simulated Space Environment on Thermal Radiation Characteristics of Selected Black Coatings. NASA TN D-4116, 1967.

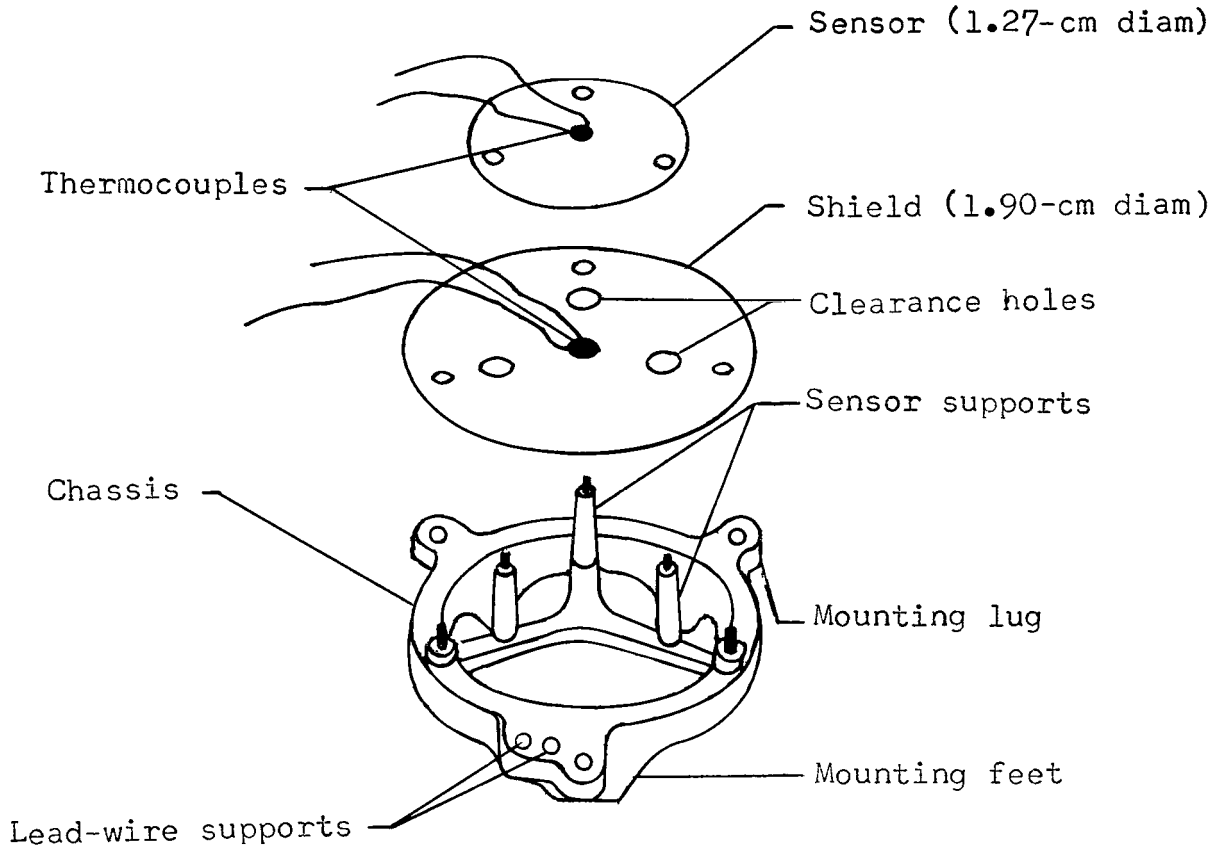

Figure 1.- Details of radiometer components.

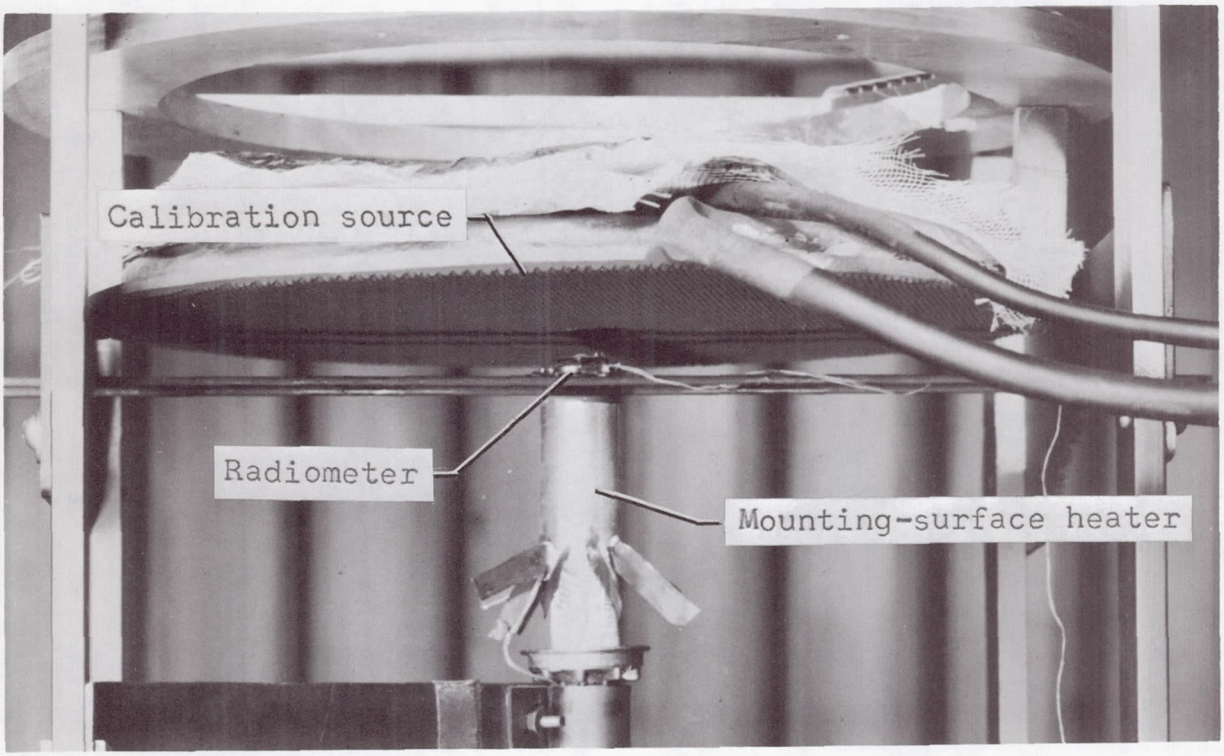

L-68-8536

Figure 2.- Calibration apparatus installed in 5-foot-diameter, 5-foot-long vacuum system at the Langley Research Center.

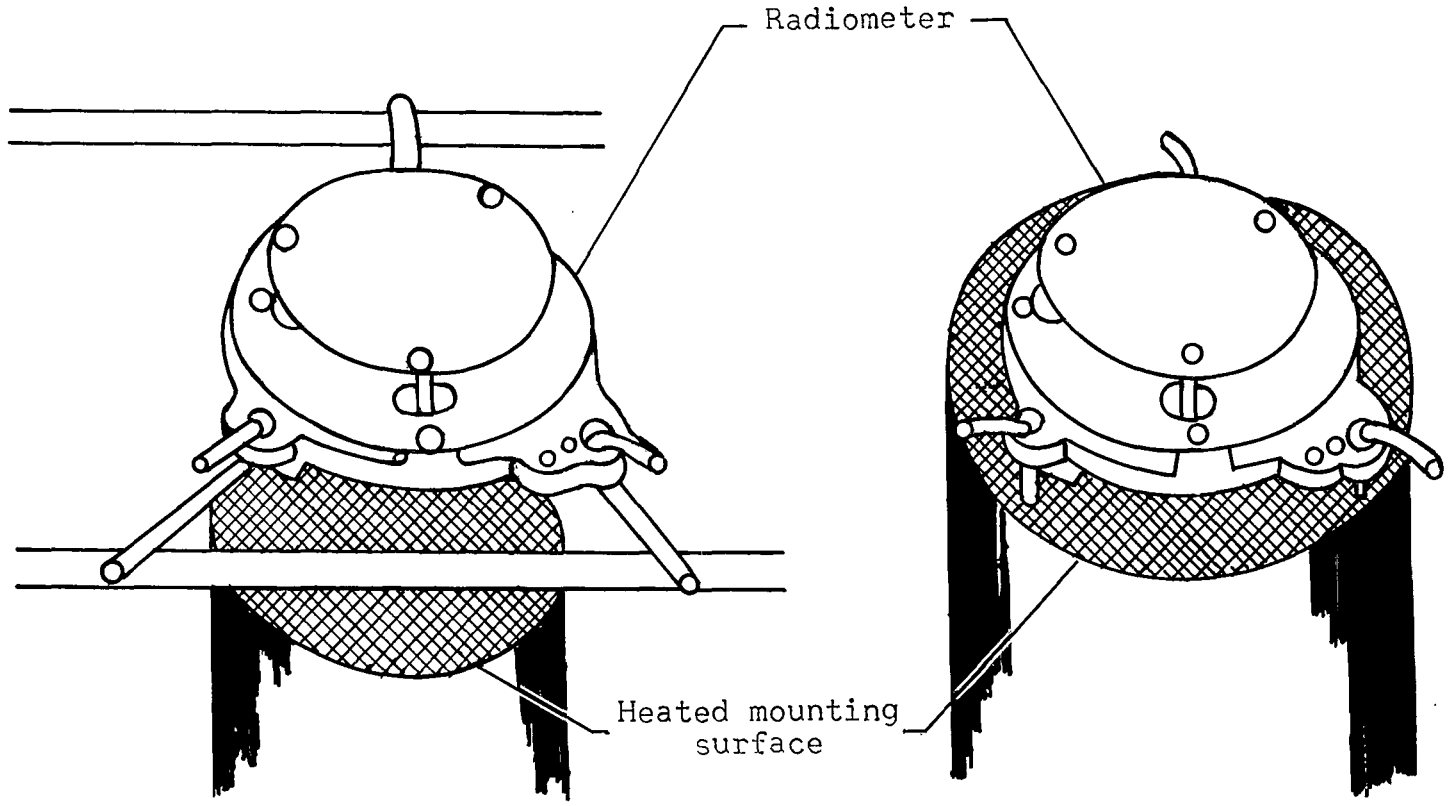

(a) Suspended mounting.

(b) Surface mounting.

Figure 3.- Radiometer mountings used for calibrations.

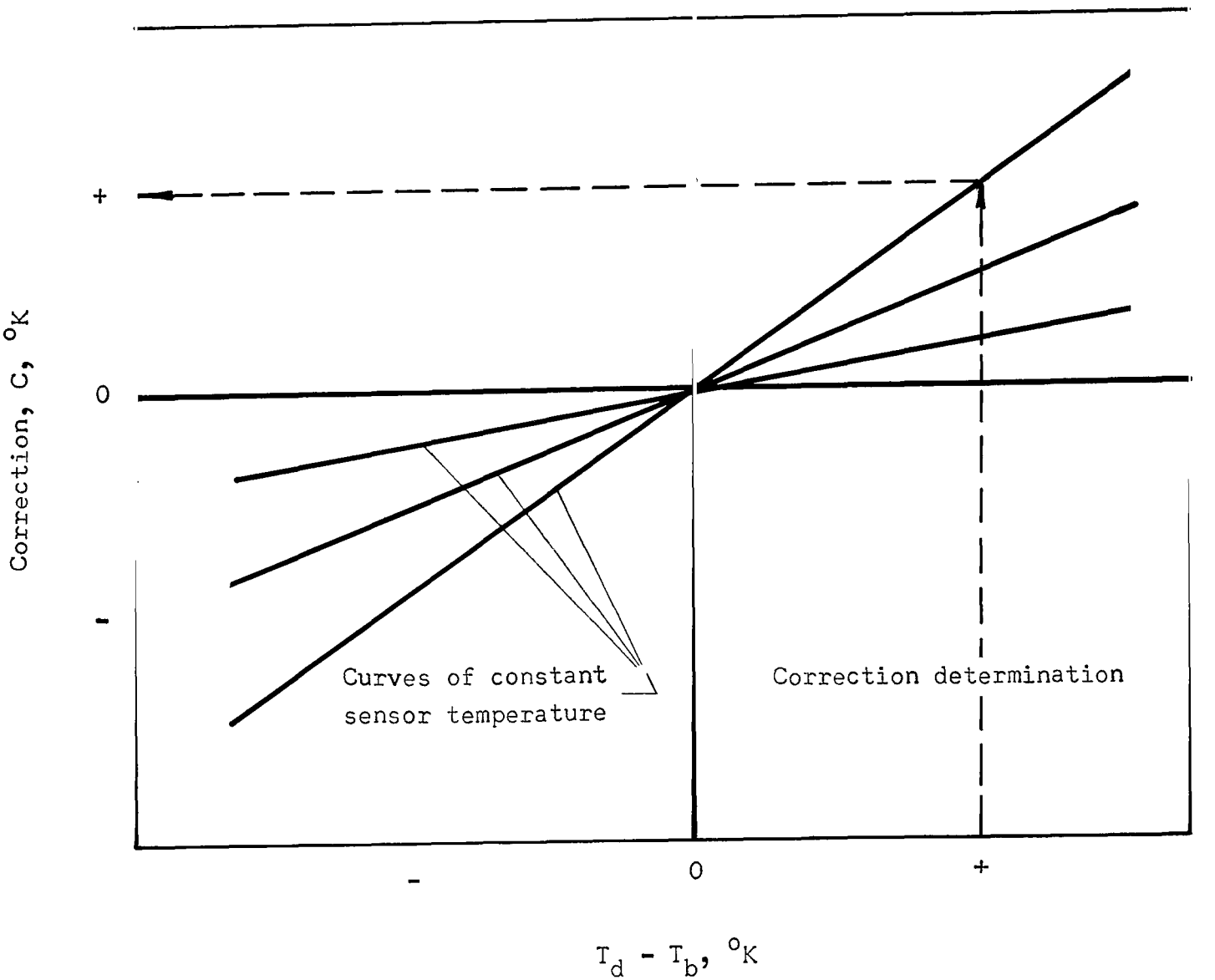

Figure 4.- Method of presenting calibration data.

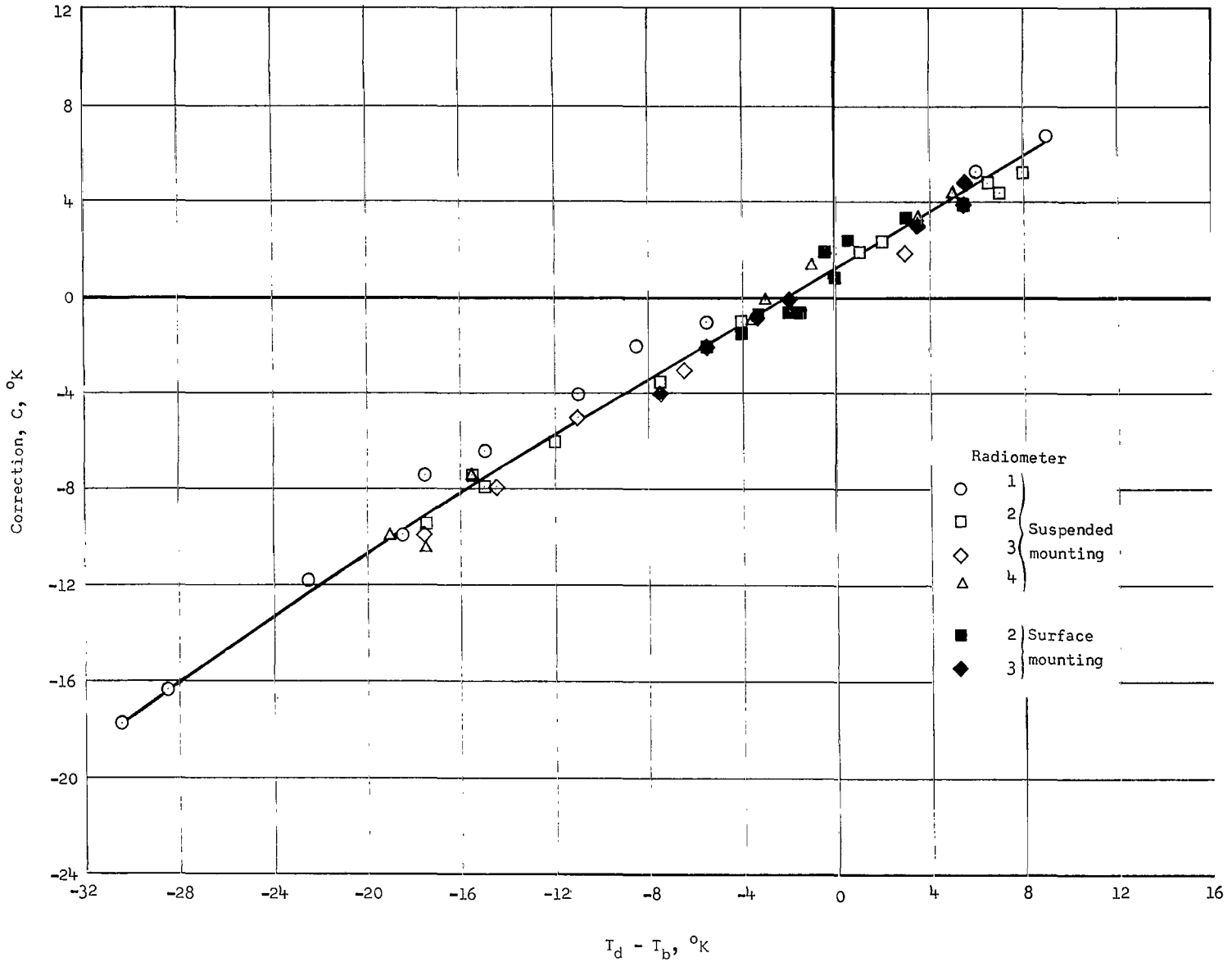

Figure 5.- Comparison of calibration results for suspended- and surface-mounted radiometers for a constant sensor temperature of 300° K.

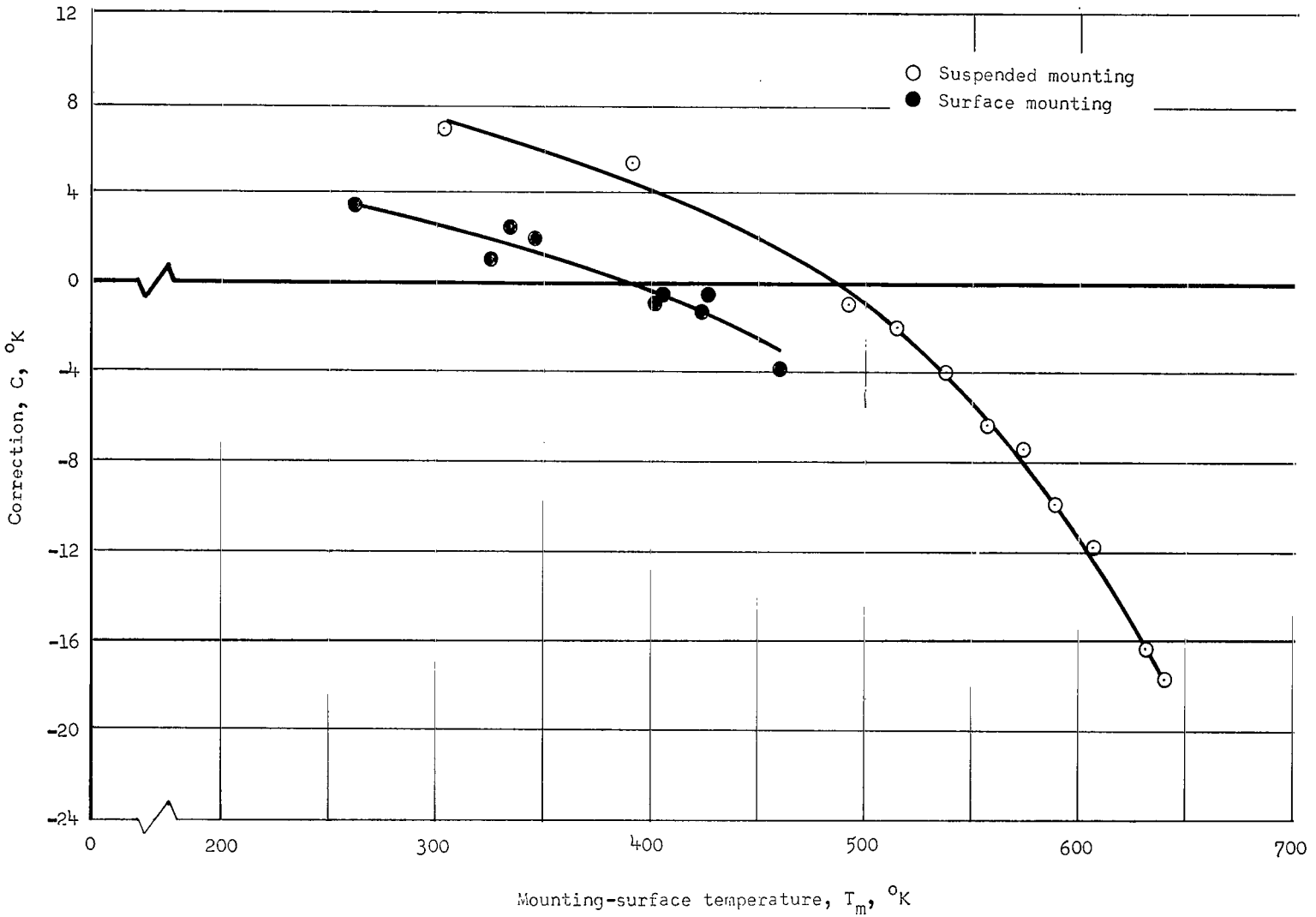

Figure 6.- Correlation of radiometer correction for test radiometer 1 with mounting-surface temperatures for a constant sensor temperature of 300° K.

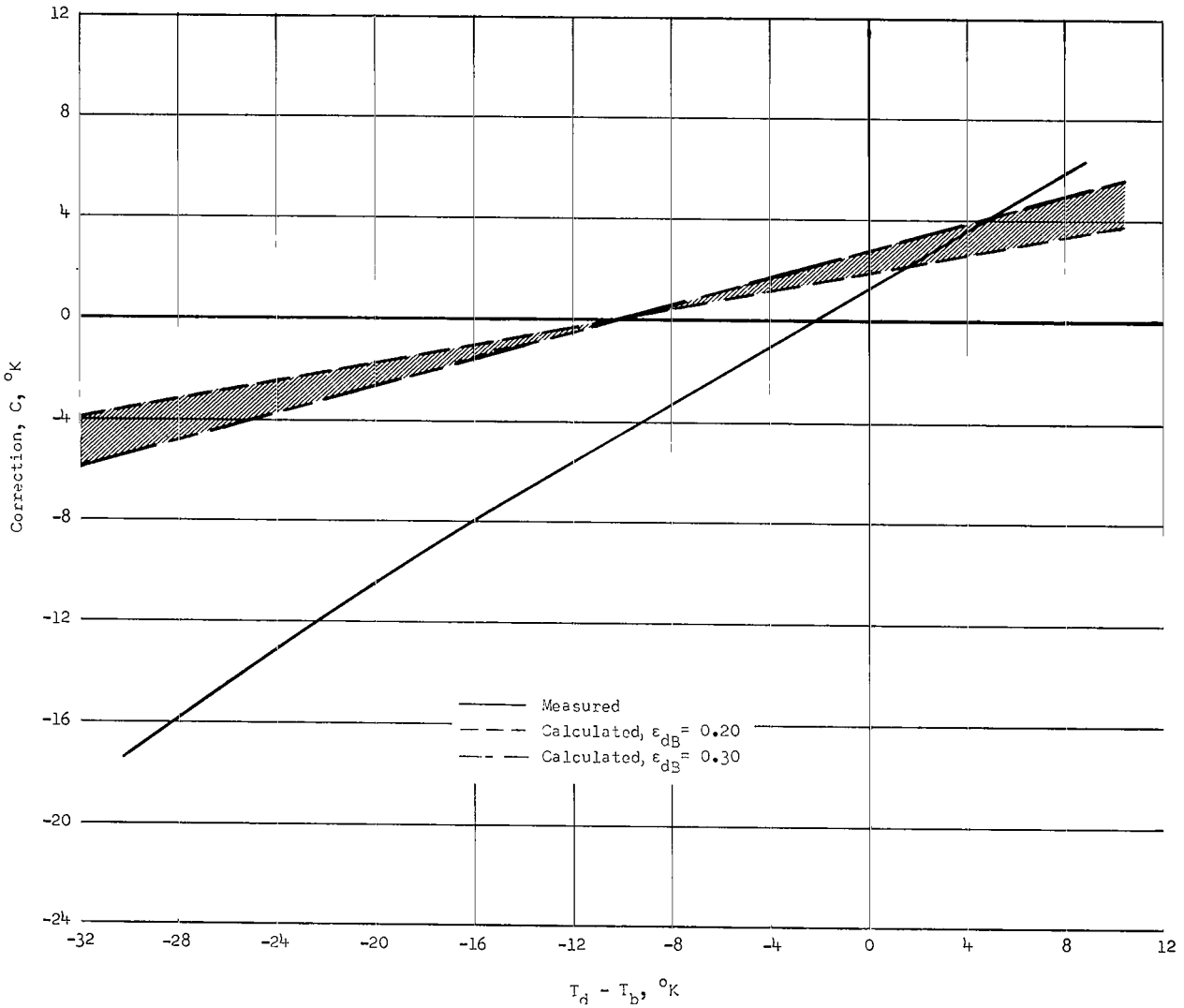

Figure 7.- Comparison of calculated calibration data, with only radiant heat transfer considered, with measured calibration data for a constant sensor temperature of 300° K.

$$C = \left[\left(1 + \frac{\varepsilon_{dB}}{\varepsilon_{dT}}\right) T_d^4 - \frac{\varepsilon_{bT} S_b}{\varepsilon_{dT} S_d} \varepsilon_{dB} F_{b,d} T_b^4\right]^{1/4} - T_d.$$

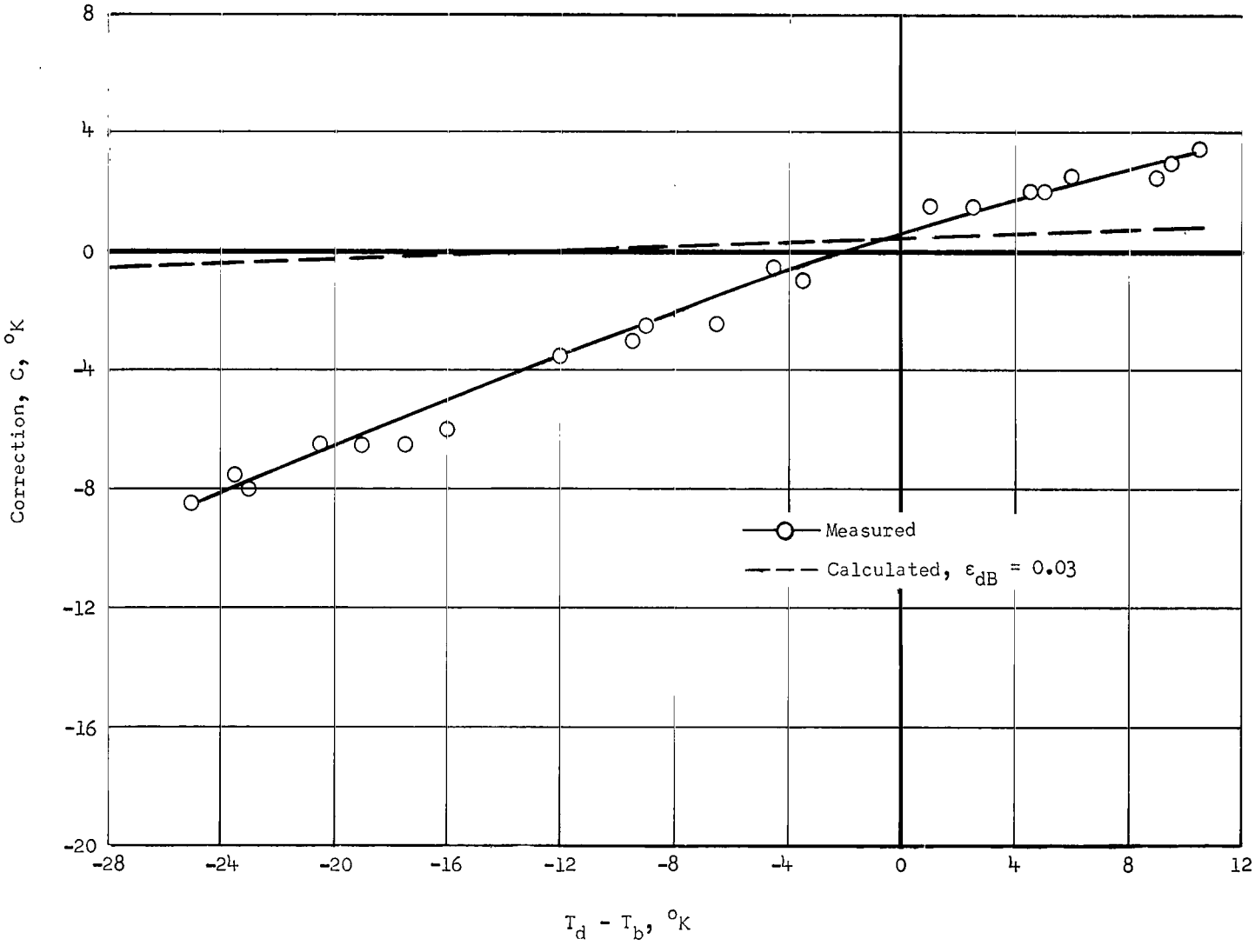

Figure 8.- Comparison of calculated calibration data, with only radiant heat transfer considered, with measured calibration data for a radiometer sensor with a low-emittance undersurface at constant sensor temperature of 300° K. $C = \left[\left(1 + \frac{\varepsilon_{dB}}{\varepsilon_{dT}}\right)T_d^4 - \frac{\varepsilon_{bT}S_b}{\varepsilon_{dT}S_d}\varepsilon_{dB}F_{B,d}T_b^4\right]^{1/4} - T_d$.

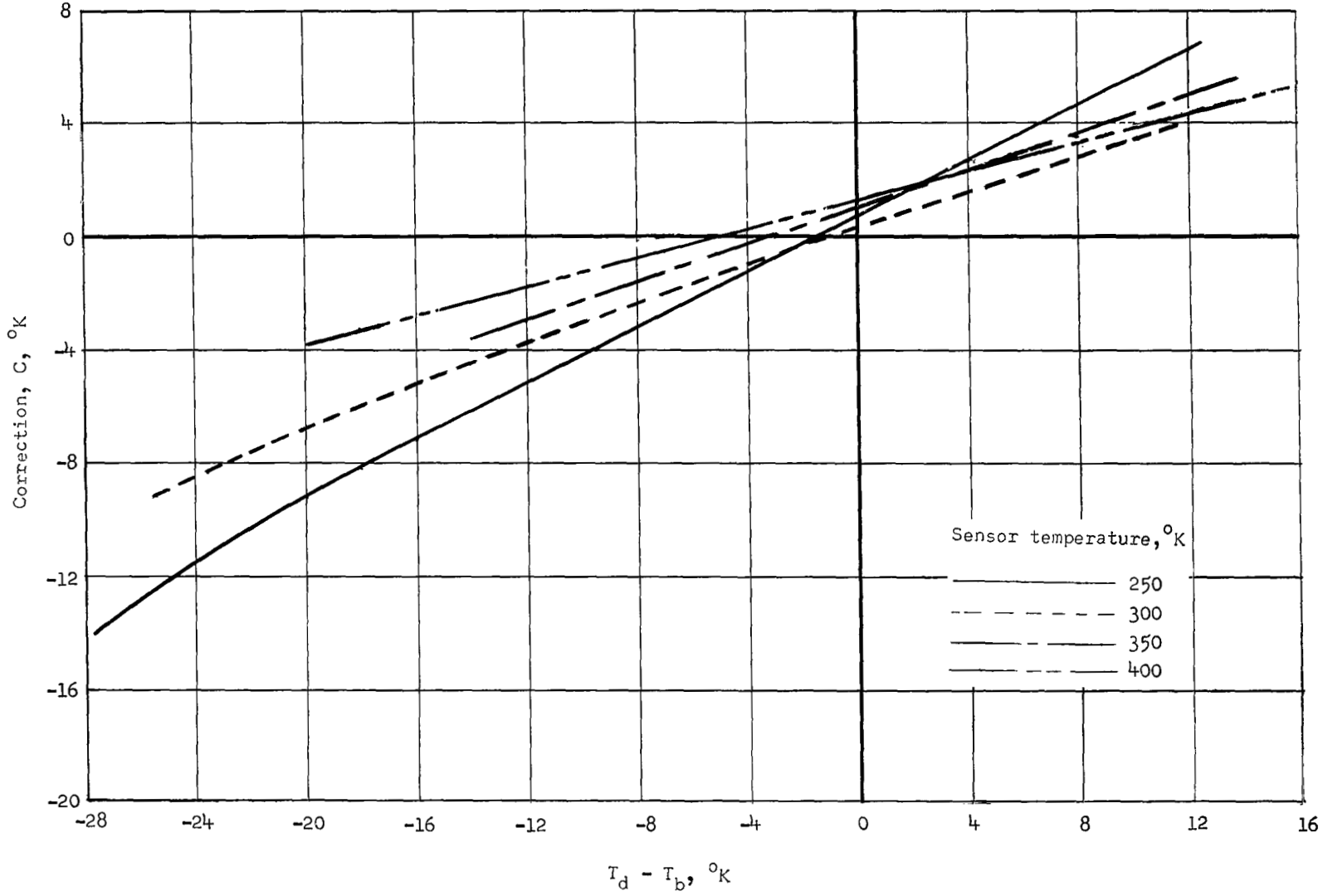

Figure 9.- Summary of measured calibration data.

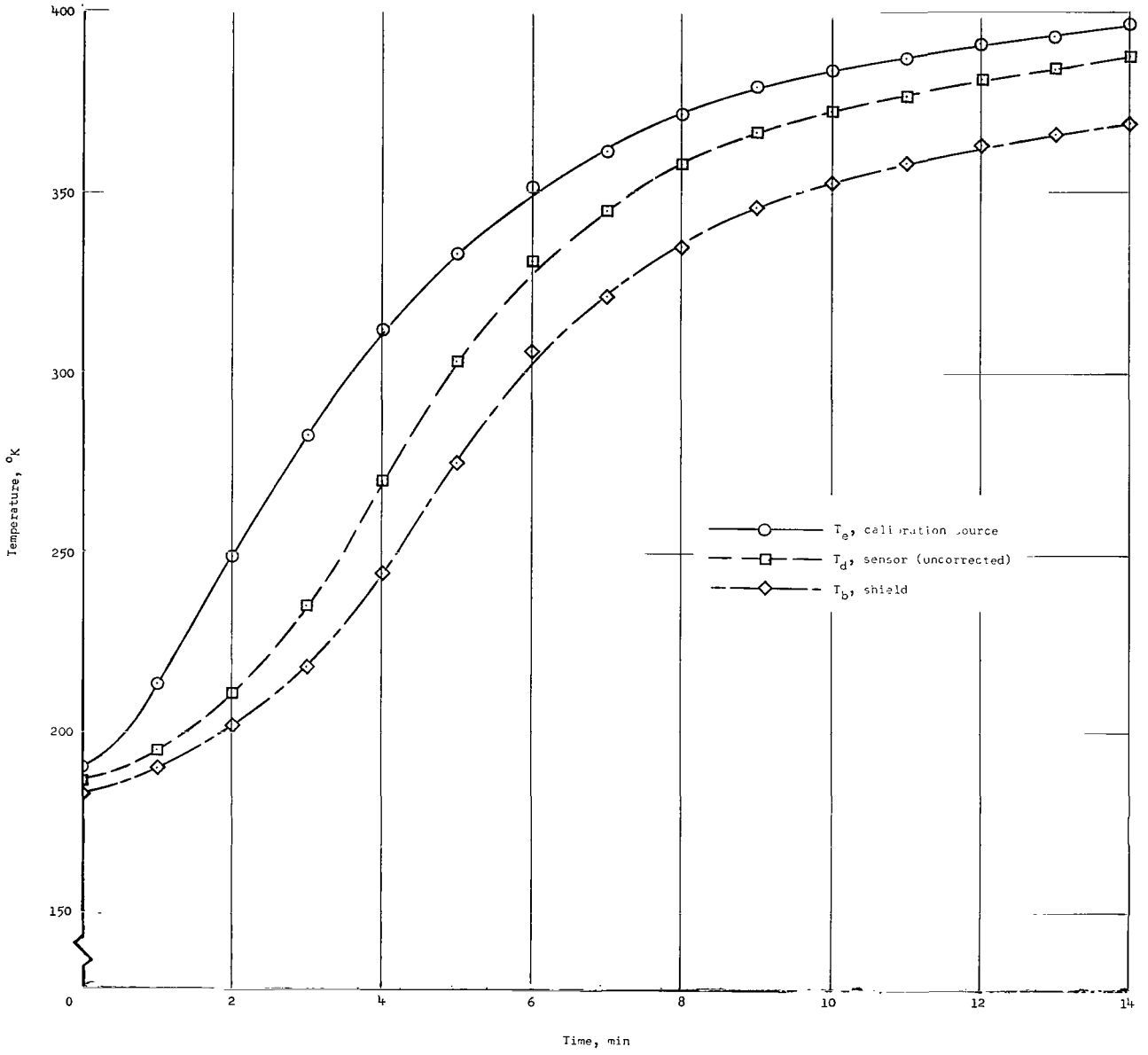

Figure 10.- Comparison of the temperature response of the radiometer sensor and shield to a rapid rise in the equivalent black-body temperature of the calibration source.

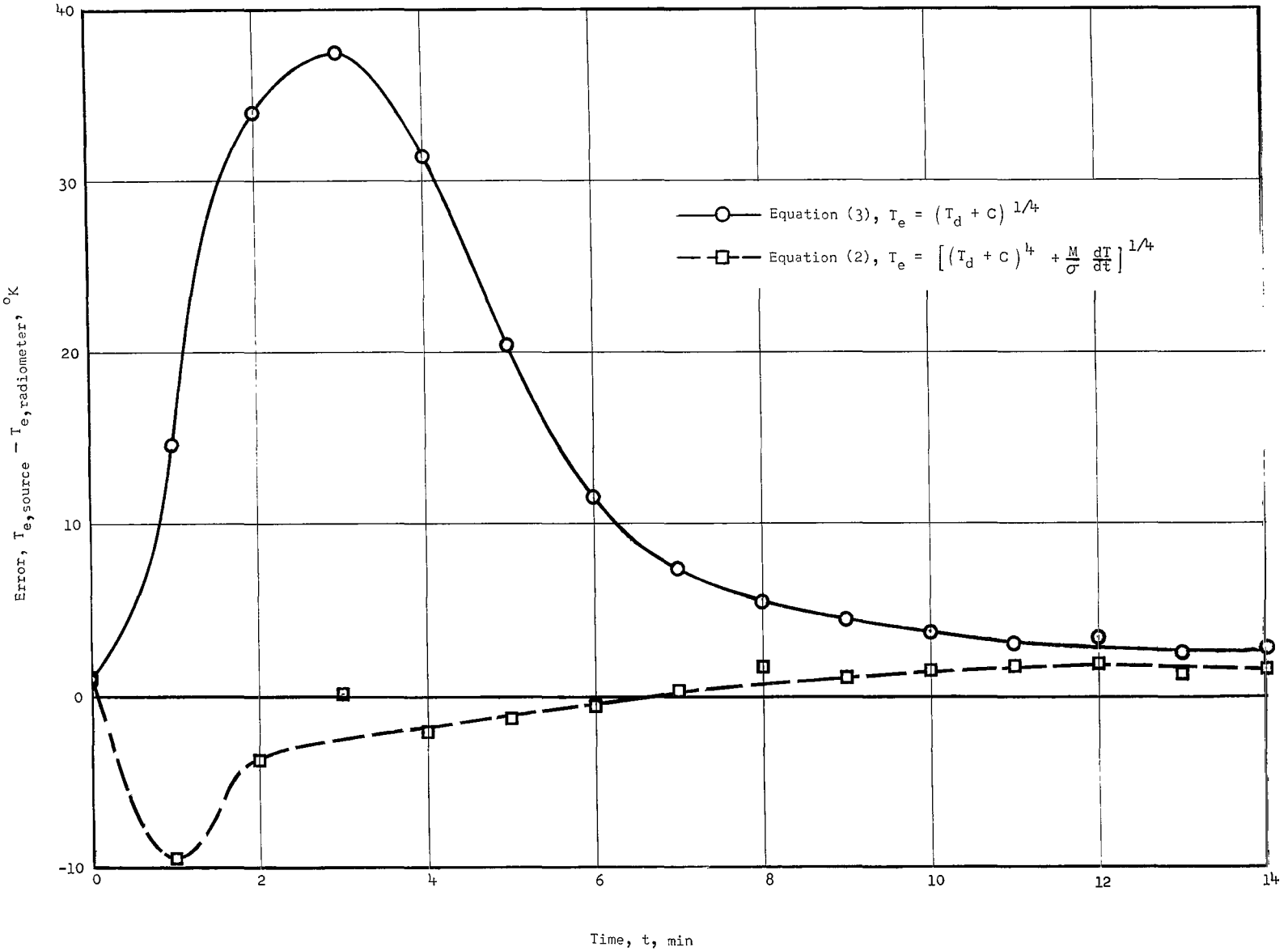

Figure 11.- Comparison of temperature differences between radiometer and calibration source for approximate (eq. (3)) and exact (eq. (2)) methods of data reduction.

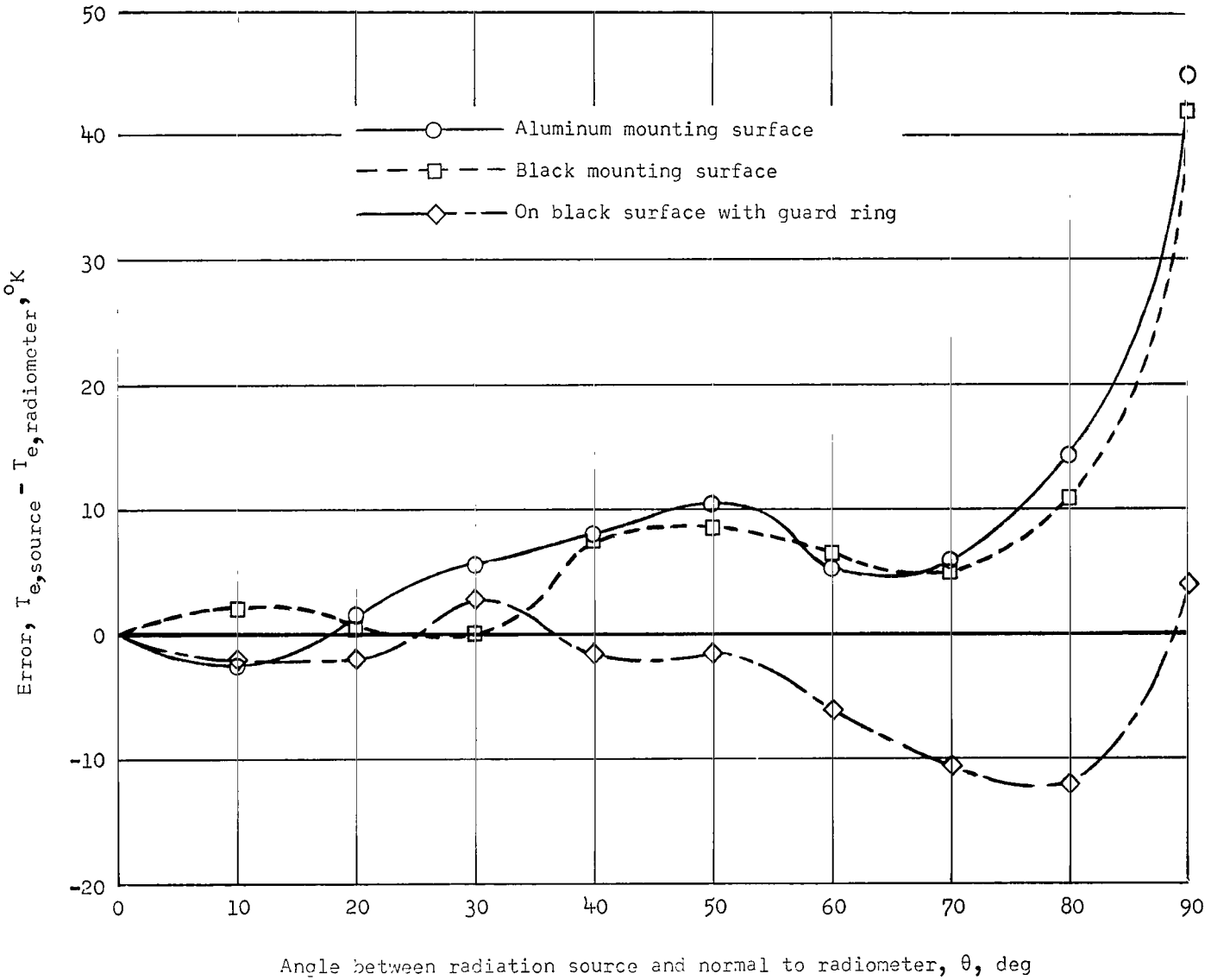

Figure 12.- Corrected radiometer readings compared with effective black-body temperature of incident irradiance for several angular positions with respect to a solar simulator and for variations in mounting surface.

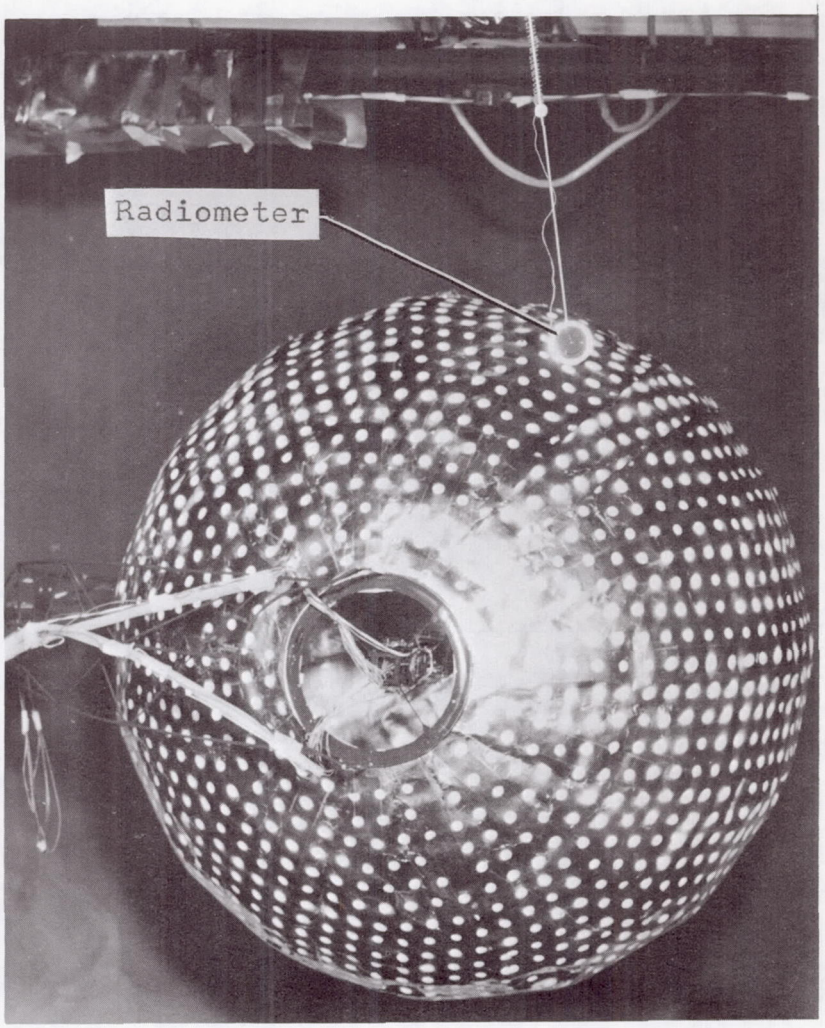

(a) Balloon model and radiometer for monitoring simulator radiance. L-68-5673

Figure 13.- Apparatus used in model balloon tests.

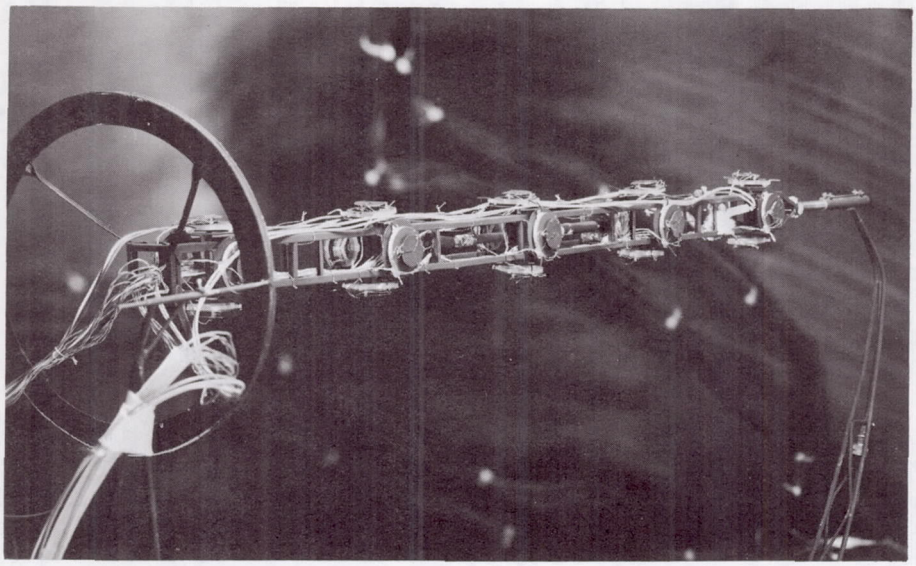

(b) Radiometer support bar.

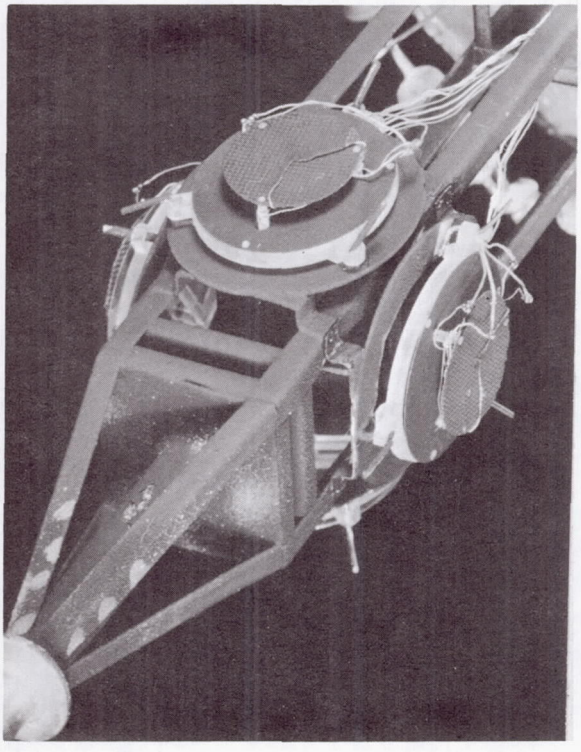

(c) Radiometer mounting detail. L-68-5674

Figure 13.- Concluded.

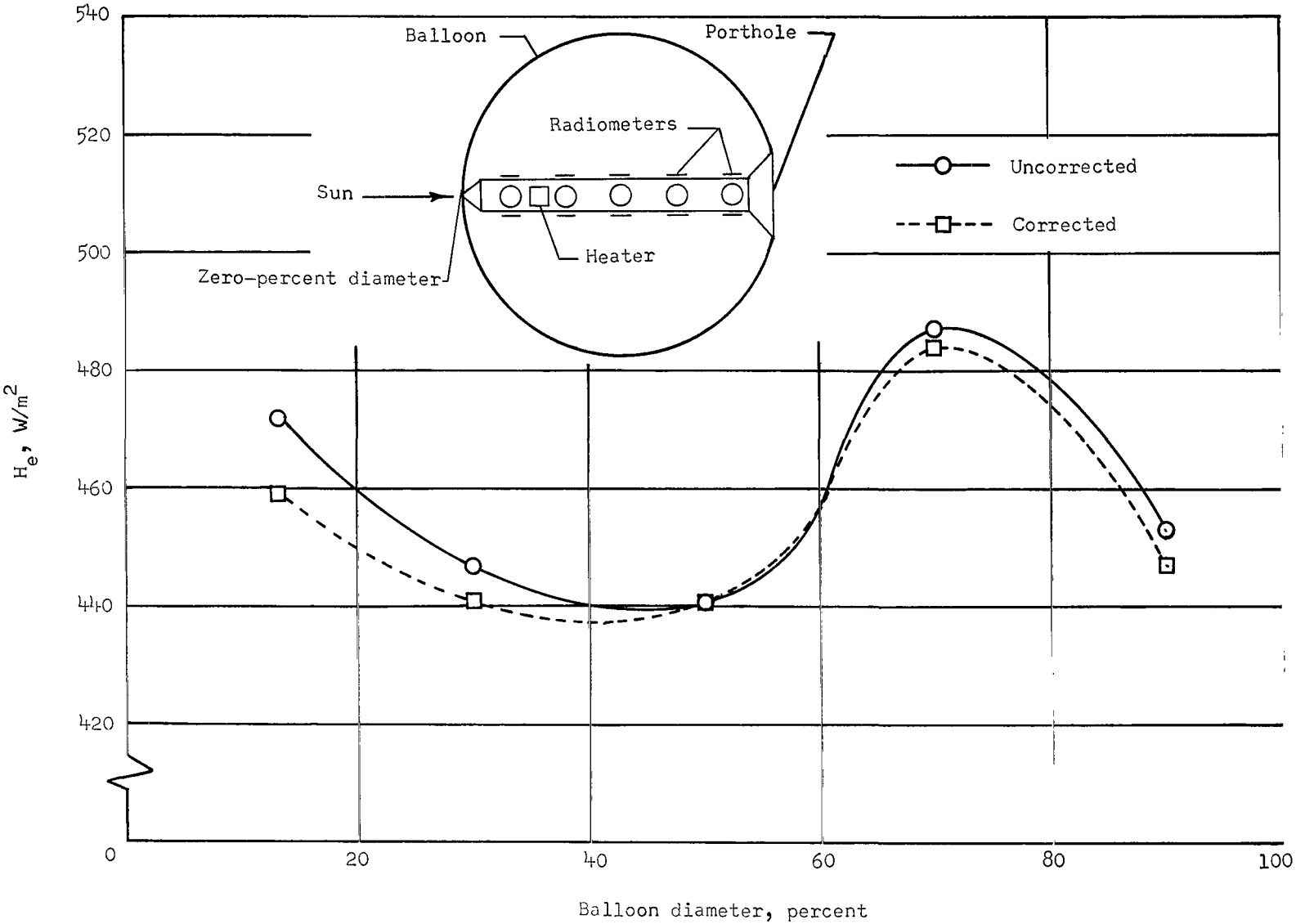

Figure 14.- Comparison of corrected and uncorrected irradiance measurements along balloon diameter.

NATIONAL AERONAUTICS AND SPACE ADMINISTRATION
WASHINGTON, D. C. 20546
OFFICIAL BUSINESS

FIRST CLASS MAIL

POSTAGE AND FEES PAID
NATIONAL AERONAUTICS AND
SPACE ADMINISTRATION

"The aeronautical and space activities of the United States shall be conducted so as to contribute . . . to the expansion of human knowledge of phenomena in the atmosphere and space. The Administration shall provide for the widest practicable and appropriate dissemination of information concerning its activities and the results thereof."

—NATIONAL AERONAUTICS AND SPACE ACT OF 1958

NASA SCIENTIFIC AND TECHNICAL PUBLICATIONS

TECHNICAL REPORTS: Scientific and technical information considered important, complete, and a lasting contribution to existing knowledge.

TECHNICAL NOTES: Information less broad in scope but nevertheless of importance as a contribution to existing knowledge.

TECHNICAL MEMORANDUMS: Information receiving limited distribution because of preliminary data, security classification, or other reasons.

CONTRACTOR REPORTS: Scientific and technical information generated under a NASA contract or grant and considered an important contribution to existing knowledge.

TECHNICAL TRANSLATIONS: Information published in a foreign language considered to merit NASA distribution in English.

SPECIAL PUBLICATIONS: Information derived from or of value to NASA activities. Publications include conference proceedings, monographs, data compilations, handbooks, sourcebooks, and special bibliographies.

TECHNOLOGY UTILIZATION PUBLICATIONS: Information on technology used by NASA that may be of particular interest in commercial and other non-aerospace applications. Publications include Tech Briefs, Technology Utilization Reports and Notes, and Technology Surveys.

Details on the availability of these publications may be obtained from:

SCIENTIFIC AND TECHNICAL INFORMATION DIVISION

NATIONAL AERONAUTICS AND SPACE ADMINISTRATION

Washington, D.C. 20546